Quantification of Steady-State Efficiency Maps vs. Time-Stepping Solutions for Drive Cycle Performance Analysis of Induction Motors

Kourosh Heidarikani*, Pawan Kumar Dhakal*, Roland Seebacher*, Annette Muetze*
*Electric Drives and Power Electronic Systems Institute, Graz University of Technology, Graz, Austria

***Abstract*—Efficiency analysis of dynamic drive cycles is crucial for evaluating electric vehicle (EV) motors. Conventional steady-state models allow fast development of efficiency maps but can lead to errors in the computation of transient performance due to grid point interpolation and the neglect of transient behavior. Limited understanding exists of the influence of grid coarseness and the error between steady-state and time-stepping solutions. This research aims to quantify these errors for a test-case laboratory-based induction motor (IM) across down-scaled drive cycles, using experimental results as a baseline. This study involves drive cycle performance derived from steady-state efficiency maps developed by finite element analysis (FEA) and direct time-stepping methods, including both analytic and FEA approaches. The results are compared with time-stepping solutions derived from laboratory measurements to identify trade-offs between computational efficiency and accuracy.**

***Index Terms*—Drive cycle performance, efficiency maps, finite element analysis (FEA), induction motor.**

I. Introduction

As energy crises and pollution intensified globally, electric vehicles (EVs) have become popular for their energy-saving and low emissions [1], [2]. This shift requires advancements in EV motor design and optimization. Drive cycles are essential in this context, as they simulate real-world driving conditions to accurately evaluate motor performance [3], [4]. Assessing motor efficiency across drive cycles enhances power-train performance, energy storage, battery management, and overall vehicle efficiency [5]. The induction motor (IM) and the permanent magnet synchronous motor (PMSM) are currently the most prevalent topologies for EV traction motors [6]. The IM offers lower cost, higher reliability, and greater robustness compared to the PMSM, and it simplifies flux weakening at high speeds due to the absence of a permanent magnetic field. Despite its disadvantages, such as lower efficiency and power factor at low speeds due to rotor copper losses, the IM is a compelling EV option for its cost-effectiveness. Optimizing IM performance across drive cycles can enhance power-train efficiency and vehicle performance, advancing cost-effective and reliable EVs [7], [8].

This work is partially supported by the joint Collaborative Research Centre CREATOR (DFG: Project-ID 492661287/TRR 361; FWF: 10.55776/F90) at TU Darmstadt, TU Graz and JKU Linz.

Efficiency maps are essential tools for evaluating the performance of EV motors across various torque-speed operating points (OPs). These maps provide valuable insights into the efficiency of the electric drive-train under different load conditions. The main techniques for calculating efficiency maps are experimental methods, finite element analysis (FEA), and analytic techniques [9]–[11]. To enhance computational efficiency and enable rapid assessments, researchers frequently use steady-state efficiency calculations to develop these look-up tables (LUTs) [12]–[14].

While LUT-based methods are efficient and streamline performance assessment, their precision may suffer due to the quality and accuracy of the input data, along with parameter uncertainties and grid coarseness [15], [16]. A significant drawback of LUT-based EMs is their inability to account for transient effects, such as dynamic changes in operating conditions. However, these factors are crucial for accurately assessing drive cycle performance in EV system design [17], [18]. Time-stepping methods, or direct approaches, can address this limitation by evaluating motor performance throughout drive cycles. However, these methods are notoriously time-consuming and require extensive computational resources, making them less practical for routine use, especially during the iterative design process of EV motors, e.g. [9], [19]. Given these complexities, comparing the efficacy of LUT-based and time-stepping methods is crucial. This comparison can reveal trade-offs between computational efficiency and accuracy, guiding researchers and engineers in selecting the best approach for evaluating the transient performance of EV motors.

This paper provides a comprehensive comparison of LUT-based methods and time-stepping solutions (model-based) for full drive cycle operations of the laboratory-scaled IM. This research quantitatively assesses the accuracy of steady-state efficiency maps and time-stepping methods through direct comparison with measurement results. A baseline study, as detailed in [17], identifies the OPs of the IM using the down-scaling method of standard drive cycles described in [20]. The primary source of comparison is the WLTP Class 3 drive cycle experimental test conducted on the IM in the laboratory. This study evaluates the errors, computational time, and accuracy of each method, highlighting their trade-offs, strengths, and weaknesses. The paper is structured as follows: Section II describes the research methodology and test case of this study. Section III discusses the performance calculation, the results of the steady-state efficiency maps, and of the direct analyses. Section IV quantifies the errors by comparing the above results directly with measurement results. Section V concludes the study with a summary of the findings.

II. Analysis Methodology and Test Case Description

A. Methodology

In this research, the performance of the target OPs of the drive cycle is quantified. Both LUT methods and time-stepping techniques are evaluated with respect to their ability to compute drive cycle performance. The time-stepping method is conducted using three different approaches: analytic, FEA, and experimental investigation. The analytic model is based on simulations in MATLAB/Simulink [21], while the FEA method is carried out using the JMAG software [22]. In the LUT-based method, only FEA is conducted to derive the efficiency map, which is then applied to build the performance map for the OPs of the drive cycle. The direct experimental investigation serves as a primary baseline for the performance assessment. The workflow of this study is presented in Fig. 1.

B. Test Case

The three-phase squirrel cage IM available in the laboratory is used for this study. The motor specifications are detailed in Table I. The analysis focuses on the Worldwide Harmonized Light Vehicles Test Procedure (WLTP) class 3 drive cycle, a standardized test used to assess light vehicle performance, shown in Fig 2. The WLTP class 3 drive cycle encompasses a broad spectrum of driving conditions. It is divided into four segments: low speed (urban), medium speed (suburban), high speed (rural), and extra high speed (highway) scenarios [23].

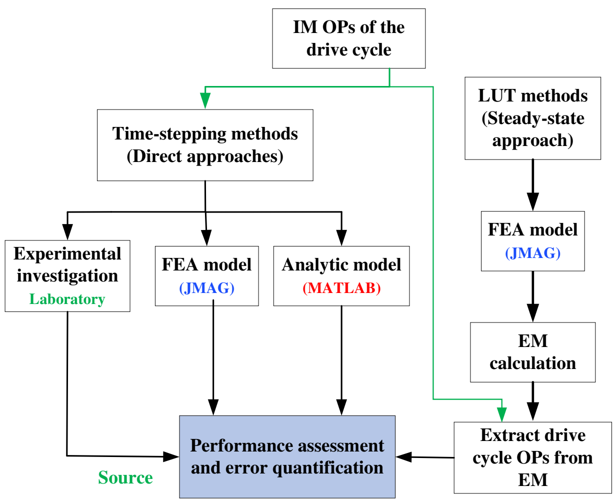

Fig. 1: Workflow of the study.

TABLE I
Laboratory Motor Specification.

Parameters	Value	Unit
Nominal power	4.4	kW
Nominal voltage	400	V rms
Nominal speed	1430	rpm
Maximum speed	2850	rpm
Nominal torque	24.7	Nm
Maximum torque	31	Nm
Number of pole pairs	2	-

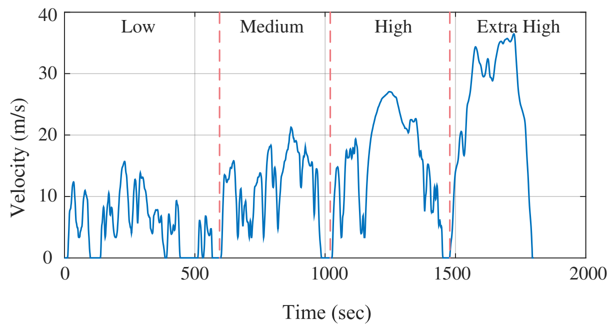

Fig. 2: WLTP class 3 drive cycle [23].

The input torque-speed OPs of the drive cycle are calculated using a quasi-steady-state (QSS) vehicle model of the BMW i3 [17]. To ensure the drive cycle OPs align with the range of the IM, the drive cycle is down-scaled according to the motor's ratings, following the methodology outlined in [20].

III. Steady-State (LUT) vs Direct Approaches

A. Steady-State Method (LUT-Based)

In the LUT-based method, the JMAG software was used for FEA. Grid patterns of 84 and 158 points were selected across the torque-speed plane of the IM. These two sets of grid points regularly spaced, covered a torque range of 0.5 Nm to 30.5 Nm and a speed range of 50 rpm to 2900 rpm. Fig. 3 shows the two sets of grid points that were used to construct the two efficiency maps. To obtain these two sets of grid points, the motor's stator current amplitudes, frequencies, and slips were initially calculated utilizing an equivalent circuit analytic model in MATLAB/Simulink using rotor field-oriented control (RFOC). These computed parameters were then used as input for the FEA simulations to determine the grid points' performances utilizing the 2D model of the IM.

Based on the power and loss results from the FEA simulation, efficiency maps were generated by performing linear interpolation on the efficiencies computed for each grid point. Since these grid points are only in the motoring region of the IM, the efficiency map for the generating region was derived by mirroring the motoring map. Fig. 4 shows the efficiency maps of the IM derived from the two sets of grid points. Efficiency values for the OPs of the down-scaled WLTP class 3 drive cycle were then extracted using these maps and MATLAB's default linear interpolation method. The resulting efficiency plots for the drive cycle OPs are displayed in Figs. 5(a,b).

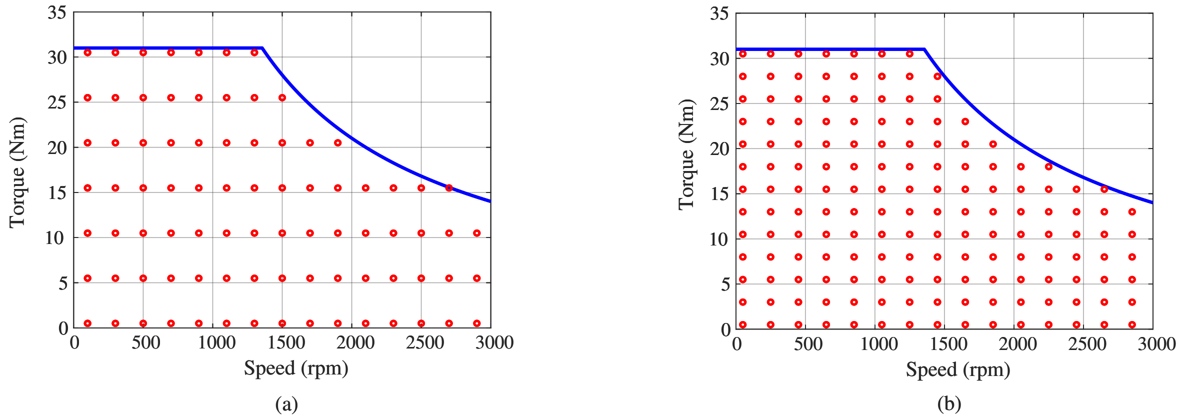

Fig. 3: Grid configurations for efficiency map generation: (a) 84 points, (b) 158 points.

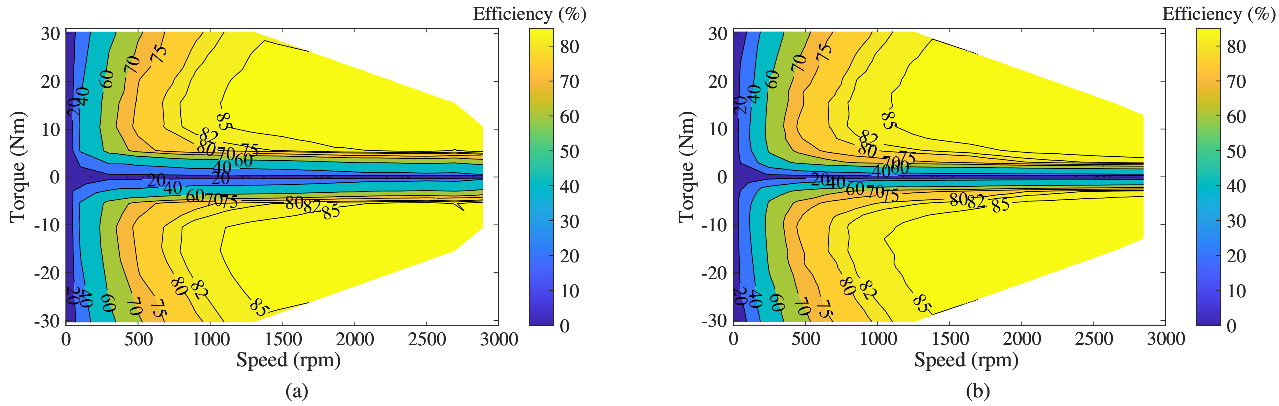

Fig. 4: Efficiency maps computed using different numbers of grid points: (a) 84 points, (b) 158 points.

B. *Direct Approach*

For the model-based direct analysis, the torque-speed OPs of the down-scaled WLTP class 3 drive cycle were simulated using both analytic and FEA approaches. This dual method ensured comprehensive validation, enhanced accuracy, and insights into model accuracy and computational time. The analytic analysis was conducted in MATLAB/Simulink, involving the development of an equivalent circuit model for the IM, using RFOC as control method, considering the laboratory test-rig limitations. The analytic model incorporates the motor equivalent circuit parameters, as well as models for iron and friction losses, both derived from experimental tests.

The direct FEA analysis utilized a 2D model of the IM. The input parameters for the direct FEA simulation were derived from the analytic simulation (similar to the case of the LUT method) to accurately achieve the OPs of the drive cycle. The performance plots of the direct FEA and analytic methods are presented in Figs. 5(c,d) respectively. To evaluate the computational efficiency, the simulation times were recorded. These simulations were conducted on a computer equipped with a 12th Gen Intel® Core™ i9-12900K processor (3200 MHz, 16 cores, 24 logical processors) and 64 GB RAM. Table II shows the simulation time for each method: The FEA analysis takes over 1.3 minutes for each OP of the IM, whereas the analytic model takes less than 300 milliseconds.

IV. Comparative Analysis with Measurement Results

To measure the down-scaled WLTP drive cycle on the IM, the test-bench depicted in Fig. 6 was employed. The IM, using RFOC consistent with the analytic and FEA models, was coupled with a PMSM machine acting as a torque-controlled load. During the drive cycle, stator voltage, current, output torque, and speed of the IM were recorded to calculate input and output power and generate efficiency plots for the OPs. Each OP was tested with a time step of 1.14 seconds, as determined by the down-scaling method applied to the drive cycle. The efficiency plot of the IM for the OPs of the drive cycle from the experimental test is shown in Fig. 7.

To assess the accuracy and error quantification of the methods in comparison with the experimental results, the root mean square error (RMSE) was employed. It

TABLE II
Simulation Time and Number Of Points in Methods.

Method	No. of OPs	Simulation time
Direct analytic	3600	12 min
Steady-state FEA (LUT)	84	115 min
Steady-state FEA (LUT)	158	3.5 hours
Direct FEA	3600	82 hours

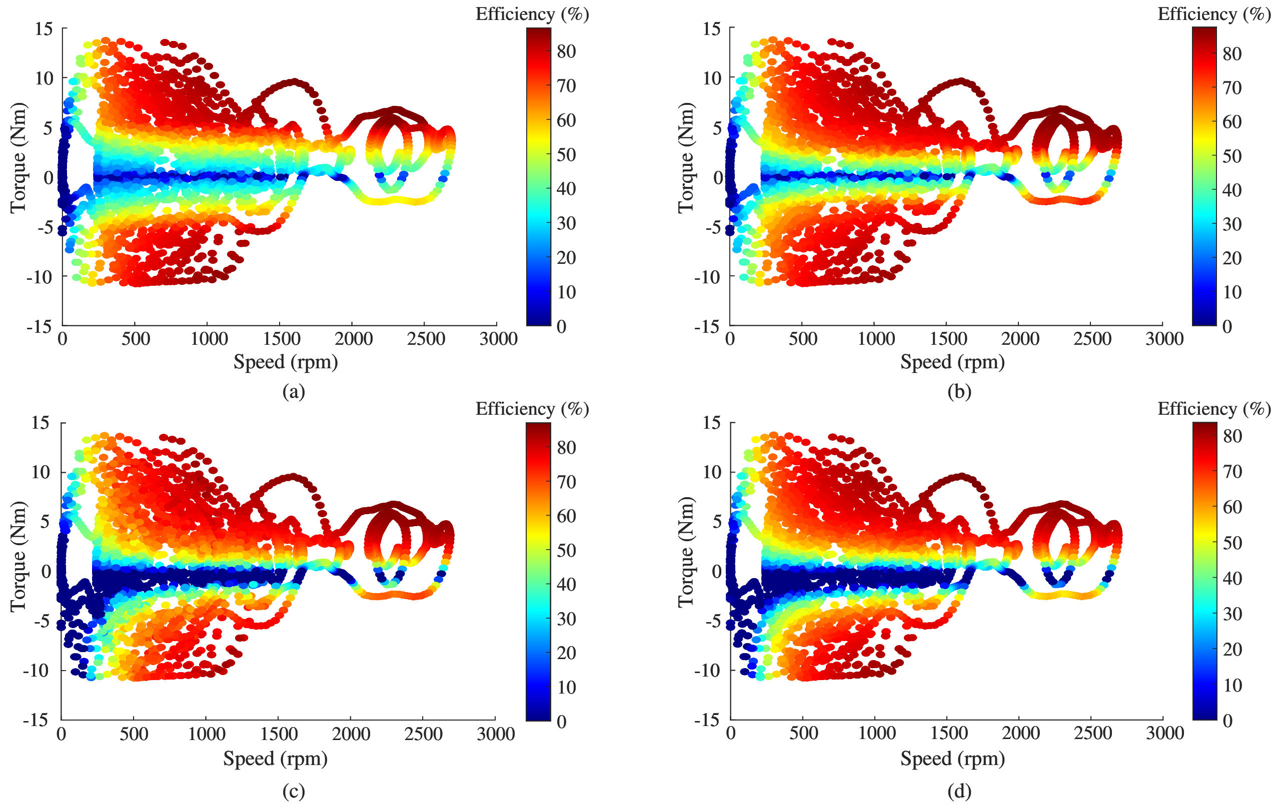

Fig. 5: Efficiency plots of the IM OPs for the down-scaled WLTP class 3 drive cycle, computed using: (a) LUT-based FEA with 84 points, (b) LUT-based FEA with 158 points, (c) direct FEA, (d) direct analytic.

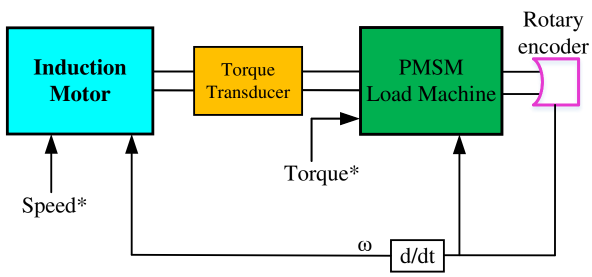

Fig. 6: Schematic of the IM test-bench in the laboratory.

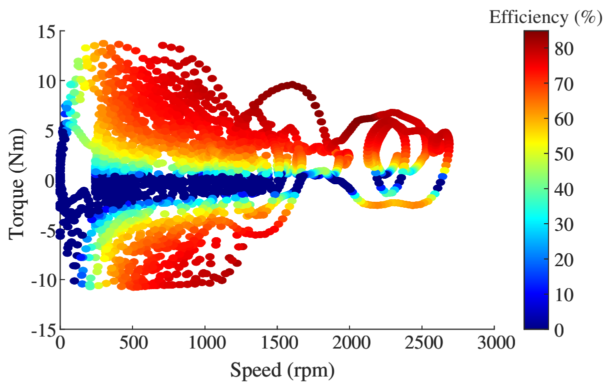

Fig. 7: Efficiency plot of the IM OPs for the down-scaled WLTP class 3 drive cycle from experimental measurement.

serves as a measure to quantify the average magnitude of discrepancies between two sets of data. It can be computed according to (1), where N represents the number of data points, m_{i} denotes the efficiency for each point from the respective methods, and s_{i} represents the efficiency from the experimental test [24].

$$\mathrm{RMSE} = \sqrt{\frac{1}{N}\sum_{i=1}^{N} |m_{\mathrm{i}} - s_{\mathrm{i}}|^2} \tag{1}$$

Table III presents the error analysis of different methods compared to the measurement results. For a detailed analysis of the WLTP drive cycle, the RMSE for each region of the drive cycle was also calculated. The following two subsections offer a comparative analysis of LUT-based and time-stepping methods across the entire drive cycle and its various regions. Additionally, they discuss the trade-offs between accuracy and computational time between the different methods.

A. *LUT-Based Method*

Considering Table III, doubling the grid points halved the error, confirming that accuracy improves with grid density and decreases the interpolation error. Meanwhile, Table II shows that the computation time nearly doubled. This emphasizes the balance between achieving greater accuracy and increasing computational time and demands.

During high-speed phases of the drive cycle, the errors are more significant compared to the low-speed, high-torque regions. In addition to interpolation errors, transient factors such as acceleration and deceleration conditions

TABLE III
ERROR ANALYSIS OF VARIOUS METHODS USING MEASUREMENT RESULTS.

Methods	Complete drive cycle	WLTP Class 3 driving phases			
		Low (Urban)	Medium (Sub-Urban)	High (Rural)	Extra-High (Highway)
Direct Analytic	3.24%	2.64%	2.19%	3.96%	3.88%
Direct FEA	5.88%	4.59%	5.06%	5.36%	7.93%
LUT FEA (84 OPs)	10.64%	7.28%	9.77%	12.23%	8.70%
LUT FEA (158 OPs)	6.26%	5.41%	5.23%	6.48%	7.37%

make efficiency prediction more complex in this method. Moreover, additional losses, especially friction losses influenced by the test-rig configuration and software constraints, which assume a linear relationship with motor speed, further increase these differences.

B. *Time-Stepping Methods*

In the direct approaches, both analytic and FEA methods show lower errors than the LUT-based methods, as expected. The analytic method demonstrated lower error compared to the FEA method. This is primarily because all losses, including friction and iron losses, were accurately modeled based on experimental data. In contrast, the FEA method exhibited higher errors, similar to those observed in the LUT method because of the way some of the loss components (i.e. friction losses) have been modeled.

Like the LUT-based methods, in the higher speed phases of the drive cycle, errors were more pronounced in both analytic and FEA methods, especially during transitions to the field weakening mode. This increased error is attributed to differences in current behavior between measurement and simulation after entering field weakening mode. In the measurements, the transition speed to field weakening is influenced by inverter limitations, whereas in the models, it is set based on the torque-speed characteristics. Moreover, there are extra losses that couldn't be accurately predicted or modeled based on the measurement tests, which contributes to the overall error in the direct comparison. The simulation times also differed significantly between the two methods. The analytic method, required much lower simulation times, making it computationally efficient. On the other hand, the FEA simulations required significantly more computational time due to the detailed electromagnetic analysis.

C. *Accuracy vs. Computation Time Trade-offs*

Based on the error analyses, the primary source of errors in both the LUT-based and the direct approaches is the inadequate modeling of the exact losses. The high computation times required for the FEA simulations in the direct approaches make them impractical for generating timely drive cycle efficiency plots. Conversely, although the direct analytic method requires less computational time and exhibits fewer errors, it notably necessitates precise modeling of friction and iron losses, ideally with the help of experimental data.

For LUT-based methods, increasing grid density beyond a certain point does not significantly reduce errors, suggesting an optimal grid density (as shown by the extreme case of the direct FEA) for acceptable accuracy in drive cycle efficiency predictions. The simulation time for the LUT-based methods is generally acceptable, and incorporating efficiency maps for different temperatures could improve drive cycle efficiency predictions. Utilizing a 3D model in FEA simulations could further enhance accuracy by capturing detailed electromagnetic end-effects, but comes at the cost of increased computational time. Therefore, while direct analytic methods offer a balance of accuracy and efficiency, LUT-based methods provide a practical alternative with acceptable accuracy, especially when optimal grid density is considered.

V. CONCLUSIONS

This study provides a comparative analysis of LUT-based and time-stepping methods for evaluating the drive cycle efficiency of a laboratory scale IM. In LUT-based methods, doubling the grid points nearly halves the overall error compared to direct measurement results. However, this error reduction becomes limited beyond a certain number of grid points. Using optimal grid density ensures these methods are efficient and accurate, although they continue to face challenges with transient effects and accurate loss modeling. Direct analytic methods, though requiring precise modeling of losses, demonstrate lower errors and computational efficiency. However, direct FEA, while offering detailed electromagnetic analysis, is computationally intensive and impractical for fast assessments. Errors in both direct methods are primarily caused by inadequate loss modeling, particularly during high-speed phases and transitions to field weakening compared to the lower speed regions in the drive cycle. Thus, while direct analytic methods balance accuracy and efficiency, LUT-based methods remain a practical alternative, particularly when considering grid density.

ACKNOWLEDGMENTS

ChatGPT 3.5 [25] has been used for editing and grammar enhancement of the paper. The paper has been subsequently edited manually again.

REFERENCES

[1] J. Wang, C. Zhang, D. Guo, F. Yang, Z. Zhang, and M. Zhao, "Drive-Cycle-Based Configuration Design and Energy Efficiency Analysis of Dual-Motor 4WD System With Two-Speed Transmission for Electric Vehicles," *IEEE Transactions on Transportation Electrification*, vol. 10, no. 1, pp. 1887–1899, Mar. 2024. [Online]. Available: https://ieeexplore.ieee.org/abstract/document/10129102

[2] Y. Cheng, Y. Wang, J. Ma, G. Liu, D. Li, and R. Qu, "Fast Evaluation of Driving Cycle Efficiency of Interior Permanent Magnet Synchronous Machines for Electric Vehicles Considering Step-Skewing," *IEEE Transactions on Industry Applications*, vol. 60, no. 3, pp. 4396–4407, May 2024. [Online]. Available: https://ieeexplore.ieee.org/document/10449412/?arnumber=10449412

[3] H. Qiu, S. Cui, S. Wang, Y. Wang, and M. Feng, "A clustering-based optimization method for the driving cycle construction: A case study in fuzhou and putian, china," *IEEE Transactions on Intelligent Transportation Systems*, vol. 23, no. 10, pp. 18 681–18 694, 2022.

[4] F. Mahmouditabar and N. J. Baker, "Design Optimization of Induction Motors with Different Stator Slot Rotor Bar Combinations Considering Drive Cycle," *Energies*, vol. 17, no. 1, p. 154, Jan. 2024. [Online]. Available: https://www.mdpi.com/1996-1073/17/1/154

[5] B. Praslicka, C. Ma, and N. Taran, "A Computationally Efficient High-Fidelity Multi-Physics Design Optimization of Traction Motors for Drive Cycle Loss Minimization," *IEEE Transactions on Industry Applications*, vol. 59, no. 2, pp. 1351–1360, Mar. 2023, s. [Online]. Available: https://ieeexplore.ieee.org/document/9942344/?arnumber=9942344

[6] "E-motors value chain," Accessed: Aug. 20, 2024. [Online]. Available: https://www.apcuk.co.uk/knowledge-base/resource/e-motors-value-chain/

[7] D. S. Yadav and M. Manisha, "Electric Propulsion Motors: A Comparative Review for Electric and Hybrid Electric Vehicles," in *2022 IEEE International Conference on Distributed Computing and Electrical Circuits and Electronics (ICDCECE)*, Apr. 2022, pp. 1–6. [Online]. Available: https://ieeexplore.ieee.org/abstract/document/9793099

[8] O. Mısır and M. Akar, "Efficiency and Core Loss Map Estimation with Machine Learning Based Multivariate Polynomial Regression Model," *Mathematics*, vol. 10, no. 19, p. 3691, Jan. 2022. [Online]. Available: https://www.mdpi.com/2227-7390/10/19/3691

[9] E. Roshandel, A. Mahmoudi, S. Kahourzade, and W. L. Soong, "Efficiency Maps of Electrical Machines: A Tutorial Review," *IEEE Transactions on Industry Applications*, vol. 59, no. 2, pp. 1263–1272, Mar. 2023. [Online]. Available: https://ieeexplore.ieee.org/abstract/document/9904865

[10] O. Stiscia, S. Rubino, S. Vaschetto, A. Cavagnino, and A. Tenconi, "Accurate Induction Machines Efficiency Mapping Computed by Standard Test Parameters," *IEEE Trans. on Ind. Applicat.*, vol. 58, no. 3, pp. 3522–3532, May 2022.

[11] R. Bojoi, E. Armando, M. Pastorelli, and K. Lang, "Efficiency and loss mapping of AC motors using advanced testing tools," in *2016 XXII International Conference on Electrical Machines (ICEM)*, Sep. 2016, pp. 1043–1049. [Online]. Available: https://ieeexplore.ieee.org/abstract/document/7732654

[12] H. Karkkainen, L. Aarniovuori, M. Niemela, and J. Pyrhonen, "Converter-Fed Induction Motor Efficiency: Practical Applicability of IEC Methods," *IEEE Industrial Electronics Magazine*, vol. 11, no. 2, pp. 45–57, Jun. 2017. [Online]. Available: https://ieeexplore.ieee.org/abstract/document/7956282

[13] H. Sano, K. Semba, Y. Suzuki, and T. Yamada, "Investigation in the accuracy of FEA Based Efficiency Maps for PMSM traction machines," in *2022 International Conference on Electrical Machines (ICEM)*. Valencia, Spain: IEEE, Sep. 2022, pp. 2061–2066.

[14] P. Ragazzo, G. Dilevrano, A. Bojoi, S. Ferrari, and G. Pellegrino, "Fast Efficiency Mapping Procedure for PMSM Accounting for the PWM Supply Impact," in *2024 IEEE International Conference on Industrial Technology (ICIT)*, Mar. 2024, pp. 1–6, iSSN: 2643-2978. [Online]. Available: https://ieeexplore.ieee.org/document/10540816/?arnumber=10540816

[15] L. di Leonardo, M. Popescu, G. Fabri, and M. Tursini, "Performance Evaluation of an Induction Motor Drive for Traction Application," in *IECON 2019 - 45th Annual Conference of the IEEE Industrial Electronics Society*. Lisbon, Portugal: IEEE, Oct. 2019, pp. 4360–4365. [Online]. Available: https://ieeexplore.ieee.org/document/8927006/

[16] S. Pastellides, S. Gerber, R.-J. Wang, and M. Kamper, "Evaluation of Drive Cycle-Based Traction Motor Design Strategies Using Gradient Optimisation," *Energies*, vol. 15, no. 3, p. 1095, Feb. 2022. [Online]. Available: https://www.mdpi.com/1996-1073/15/3/1095

[17] K. Heidarikani, P. K. Dhakal, R. Seebacher, and A. Muetze, "Baseline Determination for Drive Cycle Performance Analysis of Induction Motors," in *2023 IEEE Transportation Electrification Conference and Expo, Asia-Pacific (ITEC Asia-Pacific)*, Nov. 2023, pp. 1–6. [Online]. Available: https://ieeexplore.ieee.org/abstract/document/10372337

[18] P. K. Dhakal, K. Heidarikani, R. Seebacher, and A. Muetze, "Baseline Determination for Drive Cycle Performance Analysis of Permanent Magnet Synchronous Motors," in *2023 IEEE Transportation Electrification Conference and Expo, Asia-Pacific (ITEC Asia-Pacific)*, Chiang Mai, Thailand, Nov. 2023, pp. 1–6. [Online]. Available: https://ieeexplore.ieee.org/document/10372285

[19] M. Carbonieri, L. D. Leonardo, N. Bianchi, M. Tursini, M. A. Villani, and M. Popescu, "Cage Losses in Induction Motors Considering Harmonics: A New Finite Element Procedure and Comparison With the Time-Domain Approach," *IEEE Transactions on Industry Applications*, vol. 58, no. 2, pp. 1931–1940, Mar. 2022. [Online]. Available: https://ieeexplore.ieee.org/document/9662975/?arnumber=9662975

[20] P. K. Dhakal, K. Heidarikani, and A. Muetze, "Down-scaling of drive cycles for experimental drive cycle analyses," in *12th International Conference on Power Electronics, Machines and Drives (PEMD 2023)*, vol. 2023, Brussels, Belgium, Oct. 2023, pp. 271–276. [Online]. Available: https://ieeexplore.ieee.org/document/10324624

[21] MathWorks, "MATLAB," Accessed: Aug. 5, 2024. [Online]. Available: https://www.mathworks.com/products/matlab.html

[22] JSOL, "Simulation Technology for Electromechanical Design : JMAG," Accessed: Aug. 5, 2024. [Online]. Available: https://www.jmag-international.com/

[23] DieselNet, "Emission Test Cycles," Accessed: Aug. 6, 2024. [Online]. Available: https://dieselnet.com/standards/cycles/wltp.php

[24] D. C. Montgomery, E. A. Peck, and G. G. Vining, *Introduction to Linear Regression Analysis*. John Wiley & Sons, Feb. 2021.

[25] OpenAI, "ChatGPT 3.5," Accessed: Aug. 19, 2024. [Online]. Available: https://chatgpt.com/